

Salophen-type Macrocyclic Schiff Base Ligand and its Metal Complexes: Exploring *in vitro* Anticancer Efficacy via *in silico* Topoisomerase II α Enzyme Targeting

Monika Yadav¹, Deepak Yadav², Dharam Pal Singh¹, Jitander Kumar Kapoor^{1*}

¹Department of Chemistry, National Institute of Technology Kurukshetra-136119, Haryana, India

²Department of Experimental Medicine and Biotechnology, PGIMER, Chandigarh-160012, India

*Corresponding Author: E-mail: jkkapoor@nitkkr.ac.in

Supplementary Data

1. Experimental

1.1. Instrumentation and methods

¹H and ¹³C- NMR spectra were recorded on a Bruker AVANCE II NMR spectrometer (500 MHz) at SAIF, PU Chandigarh. FT-IR Shimadzu spectrophotometer was used for FT-IR investigations. At CIL, IIT-Jammu the HRMS study was done. EPR spectra were recorded at SAIF, IIT Bombay at room temperature, on JES-FA200 ESR Spectrometer with X band. Electronic spectra were investigated in DMSO on Duetta fluorescence and absorbance spectrophotometer. The thermal studies of all complexes were done on a Hitachi TG/DTA 7200 with a heating rate of 10°C/min. The spectrophotometric studies were performed in Tecan multimode microplate reader, infinite M200 pro (Tecan Group Ltd, Switzerland) at Central Sophisticated Instrument Cell, PGIMER, Chandigarh.

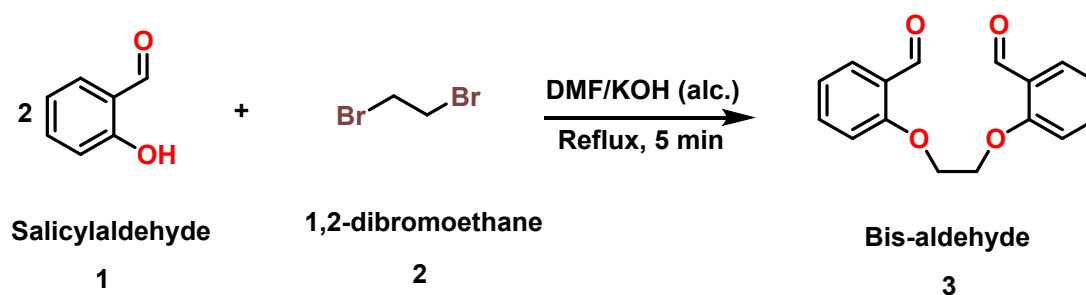
1.2. Materials

Analytical grade (AR) solvents and chemicals were directly used for this study without further purification. Bis-aldehyde **3** was prepared according to published literature as shown in ESI (**Scheme S1**)¹. 5-Bromo-2,3-diaminopyridine was ordered from TCI chemicals. All the metal salts used in synthesis were procured from Loba Chemie and Avra Synthesis Co.

1.3. Synthesis of Bis-aldehyde **3**

Salicylaldehyde (20 mM) was treated with ethanolic KOH (prepared by dissolving 1.12 g, 20 mM, of KOH in 20 mL of absolute ethanol). The solvent was removed under reduced pressure, and the resulting potassium salt was dissolved in 15 mL of DMF. 1,2-Dibromoethane (10 mM) was added, and the mixture was refluxed for 10 min, during which KBr precipitated. The completion of reaction was observed by TLC. The reaction mixture was cooled down to room temperature and poured on crushed

ice, the product precipitated out. The required product filtered and washed with water, dried in vacuo and purified by column chromatography. Yield: 90%, FT-IR (KBr, cm^{-1}): 3109 (Ar-H), 1685 (C=O), 1597 (C=N) (**Figure S1**). ^1H NMR (500 MHz, DMSO d_6); δ (ppm) 10.32 (2H, d), 7.69 (4H, m), 7.34 (2H, dt), 7.11 (2H, tt), 4.60 (4H, s), 7.19 (**Figure S2**). ^{13}C NMR (500 MHz, DMSO d_6); δ (ppm) 189.01, 160.72, 136.24, 127.46, 124.46, 121.01, 114.07, 67.33 (**Figure S3**).



Scheme S1. The schematic representation of synthesis of Bis-aldehyde **3**.

1.4. Synthesis of Schiff base (**4**)

A solution of bis-aldehyde **3** (5 mM) in dry methanol was added in solution of 5-Bromo-2,3-diaminopyridine (5 mM) in same solvent dropwise. The resulting reaction mixture was refluxed for 3 hrs under nitrogen atmosphere. The completion of reaction was confirmed by TLC. The reaction mixture was cooled down and the yellow solid was filtered and dried under vacuo. The purification of ligand was done by column chromatography. Yield: 80%, HRMS m/z : $[\text{M}]^+$ calcd, 422.2820; found $[\text{M}]^+$, 422.0506 (**Figure S9**). FT-IR (KBr, cm^{-1}): 3142 (Ar-H), 1604 (C=N) (**Figure 1**). ^1H NMR (500 MHz, DMSO d_6); δ (ppm) 8.76 (2H, s), 8.14 (2H, dd), 7.86 (1H, d), 7.5 (2H, m), 7.3 (2H, dd), 7.19 (1H, d), 7.02 (2H, d), 4.6 (4H, s) (**Figure 2**). ^{13}C NMR (500 MHz, DMSO d_6); δ (ppm) 158.77, 155.32, 153.96, 145.40, 136.16, 133.26, 132.45, 127.78, 124.77, 124.19, 121.02, 113.69, 105.11, 68.0 (**Figure S8**). Anal. Calcd for $\text{C}_{21}\text{H}_{16}\text{BrN}_3\text{O}_2$: C, 59.73; H, 3.82; N, 9.95; Found: C, 60.12; H, 4.24; N, 9.45.

1.5. Synthesis of metal complexes (**5a-5d**)

The Schiff base ligand **4** (2 mM) was dissolved in MeOH: DMF (1:1) and metal salts (2 mM) were added by dissolving in methanol. The resulting mixture was refluxed for 8-10 hrs. The complexes were precipitated and filtered off. The solid residue washed by diethyl ether and dried under vacuo.

$[\text{Zn}(\text{C}_{21}\text{H}_{16}\text{BrN}_3\text{O}_2)(\text{NO}_3)_2]$ (**5a**): Yield: 45%, HRMS m/z : $[\text{M}]^+$ calcd, 608.9474; found $[\text{M}+1]^+$, 609.007 (**Figure S10**). FT-IR (KBr, cm^{-1}): 3068.82 (Ar-H), 1604.77 (C=N), 597 (M-N) (**Figure S4**). Anal. Calcd for $[\text{Zn}(\text{C}_{21}\text{H}_{16}\text{BrN}_3\text{O}_2)(\text{NO}_3)_2]$: C, 41.24; H, 2.64; N, 11.45; Found: C, 42.09, H, 2.53; N, 11.21.

[Cu(C₂₁H₁₆BrN₃O₂) (NO₃)₂] (**5b**): Yield: 50%, HRMS m/z: [M]⁺ calcd, 607.9478; found [M-1]⁺, 606.993 (**Figure S11**). FT-IR (KBr, cm⁻¹): 3068.75 (Ar-H), 1600.92 (C=N), 596 (M-N) (**Figure S5**). Anal. Calcd for [Cu(C₂₁H₁₆BrN₃O₂) (NO₃)₂]: C, 43.36; H, 2.64; N, 11.48; Found: C, 43.95; H, 2.33; N, 11.05.

[Co(C₂₁H₁₆BrN₃O₂) (NO₃)₂] (**5c**): Yield: 65%, HRMS m/z: [M]⁺ calcd, 607.940; found [M]⁺, 607.058 (**Figure S12**). FT-IR (KBr, cm⁻¹): 3068.75 (Ar-H), 1600.92 (C=N), 597 (M-N) (**Figure S6**). Anal. Calcd for [Co(C₂₁H₁₆BrN₃O₂) (NO₃)₂]: C, 41.68; H, 2.66; N, 11.57; Found: C, 42.13; H, 3.01; N, 11.96.

[Ni(C₂₁H₁₆BrN₃O₂) (NO₃)₂] (**5d**): Yield: 45%, HRMS m/z: [M]⁺ calcd, 602.950; found [M+5H]⁺, 607.062 (**Figure S13**). FT-IR (KBr, cm⁻¹): 3064.89 (Ar-H), 1602 (C=N), 596 (M-N) (**Figure S7**). Anal. Calcd for [Ni(C₂₁H₁₆BrN₃O₂) (NO₃)₂]: C, 41.69; H, 2.17; N, 11.58; Found: C, 41.11; H, 2.67; N, 12.22.

1.6. Computational studies

DFT calculations were performed to optimize the geometric structures of the synthesized compounds using Gaussian 09W package². Geometry optimization was carried out employing the B3LYP functional in the conjunction with the 6-311G (d, p) and LANL2DZ basis sets. Furthermore, the energies of the frontier molecular orbitals (FMOs), specifically lowest unoccupied molecular orbital (LUMO) and the highest occupied molecular orbital (HOMO), were computed using the same computational method. All relevant chemical parameters for the metal complexes were subsequently determined based on this level of theory and the established equations from our previously reported paper³.

1.7. Molecular docking

The inhibitory activity of the complexes **5a-5d** and ligand **4** against cancer related target Topoisomerase II β enzyme protein [PDB: 4G0V] was assessed using molecular docking simulations. AutoDock Vina and GOLD software were used for docking, and Discovery Studio Visualizer v21.1.0.20298 aided was used in visualizing the ligand-protein complex^{4,5}. The PDB and sdf files of the synthesized compounds were generated from the optimized structure of each respective molecule and the PDB file of protein was downloaded from RCSB.

1.8. Biological efficacy

1.8.1. Cell culture

The human liver cancer cell line HepG2 (ATCC HB-8065) was purchased from the American Type Culture Collection (ATCC) for *in vitro* cytotoxicity assays. Cells were maintained in T-25 flasks containing high-glucose Dulbecco's Modified Eagle Medium (DMEM; 9 g/L), supplemented with 4.5

g/L glucose, 10% fetal bovine serum (FBS), 1 mM sodium pyruvate, 4 mM L-glutamine, 1.5 g/L sodium bicarbonate, 130 mg/L penicillin, and 70 mg/L streptomycin. The culture medium also included a trace amount of phenol red as a pH indicator. Flasks were incubated in a humidified atmosphere at 37°C with 5% CO₂⁶.

1.8.2. Trypan blue assay

Cell viability was assessed at 80% confluence using the Trypan blue exclusion assay. Briefly, the culture medium was aspirated, and adherent cells were detached by trypsinization. Following detachment, cells were washed twice with phosphate-buffered saline (PBS) to remove residual trypsin. The cells were then diluted 1:1 with a Trypan blue solution (1:1 in PBS) for staining. Viable cells with intact membranes reject the dye, whereas non-viable cells with broken membranes absorb the stain, resulting in a distinct blue cytoplasm. The number of viable and non-viable cells was manually determined by using a haemocytometer under an inverted microscope. This assay provided a quantitative measure of cell health and proliferation for subsequent cytotoxicity analysis⁷.

1.8.3. 3-(4,5-Dimethylthiazol-2-yl)-2,5 Diphenyltetrazolium Bromide (MTT) assay (Qualitative Assay for Determining Cytotoxicity)

Cell viability was assessed by using MTT assay, which measures mitochondrial activity as an indicator of living cells⁸. HepG2 cells were seeded at a density of 4×10³ cells per well in 96-well plates and left to adhere until reaching 80% confluence (1-2 days). After washing twice with PBS to remove residual culture medium, the compounds were diluted in culture media with 1:1 (v/v) mixture of DMSO and ethanol, ensuring a final solvent concentration below 0.1% to minimize solvent effects. The media was removed after a 24-hrs incubation with various compound concentrations and cells were washed twice with PBS. Subsequently, 10 µL of MTT solution (5 mg/mL) and 90 µL of fresh culture media were added to each well. The plates were incubated for 4 hrs at 37°C in the dark to allow for formazan crystal formation in viable cells. The supernatant was then discarded, and the cells were washed twice with PBS. To solubilize the formazan crystals, 100 µL of DMSO was added to each well, and the plate was shaken for 10 minutes. Cell viability quantified by measuring absorbance at 570 nm using an ELISA plate reader. The percentage of the cell viability for each compound was calculated relative to an untreated control using formula:

$$\text{Inhibition (\%)} = 100 - [(\text{Test OD}/\text{Control OD}) \times 100]$$

(OD = Optical Density)

The experiment was performed in triplicate for each concentration, and cytotoxicity was determined based on the mean absorbance values. This assay provided a quantitative assessment of the cytotoxic effects of the synthesized compounds on the HepG2 cell line.

1.8.4. Haemolytic assay

The haemolytic potential of the synthesized compounds on human red blood cells (hRBCs) was evaluated using a haemolysis assay. Fresh whole blood, collected in heparinized tubes, was centrifuged at 2500 rpm for 5 minutes to isolate the RBC pellet. To remove residual plasma components, the RBCs were washed with a 150 mM saline solution. After washing, the RBCs were resuspended in pH-adjusted 100 mM phosphate buffer at a 1:10 dilution, resulting in a final concentration of approx. 1.08×10^8 RBCs/mL.

For the haemolysis assay, 800 μ L of phosphate buffer, 500 μ L of serially diluted test compound solutions, and 200 μ L of the diluted RBC suspension were combined in Eppendorf tubes. The mixtures were incubated at 37°C in a shaking water bath for 1 hour to allow haemolytic compounds to induce haemoglobin release. Following incubation, centrifugation at 13,500 g for 5 minutes separated intact RBCs (pellet) from the released haemoglobin in the supernatant. The absorbance of the supernatant, indicative of haemoglobin concentration and thus haemolytic activity, was measured at 540 nm using a spectrophotometer.

Phosphate buffer (minimal haemolysis) served as the negative control, and Triton X-100 (100% haemolysis), a known haemolytic agent, served as the positive control. The percentage of haemolysis induced by the test compounds was calculated using the formula:

$$\% \text{ Haemolysis} = [(\text{Test OD} - \text{Negative Control OD}) / (\text{Positive Control OD} - \text{Negative OD})] \times 100.$$

This assay provided a quantitative assessment of the haemolytic potential of the synthesized compounds on human RBCs³.

References:

1. M. M. H. Khalil, E. H. Ismail, G. G. Mohamed, E. M. Zayed and A. Badr, *OJIC*, 2012, 02, 13–21.
2. I. Piyanzina, B. Minisini, D. Tayurskii and J.-F. Bardeau, *J Mol. Model.*, 2015, **21**, 34.
3. M. Yadav, D. Yadav, S. Kansal, A. Angrup, N. Taneja, D. P. Singh and J. K. Kapoor, *J. Mol. Struct.*, 2024, **1317**, 139078.
4. B. Lal, R. K. Tittal, R. S. Mathpati, G. Vikas D, N. Nehra and K. Lal, *J. Mol. Struct.*, 2023, **1294**, 136455.

5. B. Lal, V. Kumar, R. K. Tittal, R. S. Mathpati and P. Chetti, *J. Mol. Struct.*, 2025, **1326**, 141092.
6. P. Thapa, R. Karki, U. Thapa, Y. Jahng, M.-J. Jung, J. M. Nam, Y. Na, Y. Kwon and E.-S. Lee, *Bioorg. Med. Chem.*, 2010, **18**, 377–386.
7. L. J. Lalitha, T. J. Sales, Prince.P.Clarence, P.Agastian, Y.-O. Kim, A. H. Mahmoud, S. E. Mohamed, J. C. Tack, S. W. Na and H.-J. Kim, *J. King Saud Univ. – Sci.*, 2020, **32**, 1246–1253.
8. F. Piccinini, A. Tesei, C. Arienti and A. Bevilacqua, *Bio. Proced. Online*, 2017, **19**, 8.

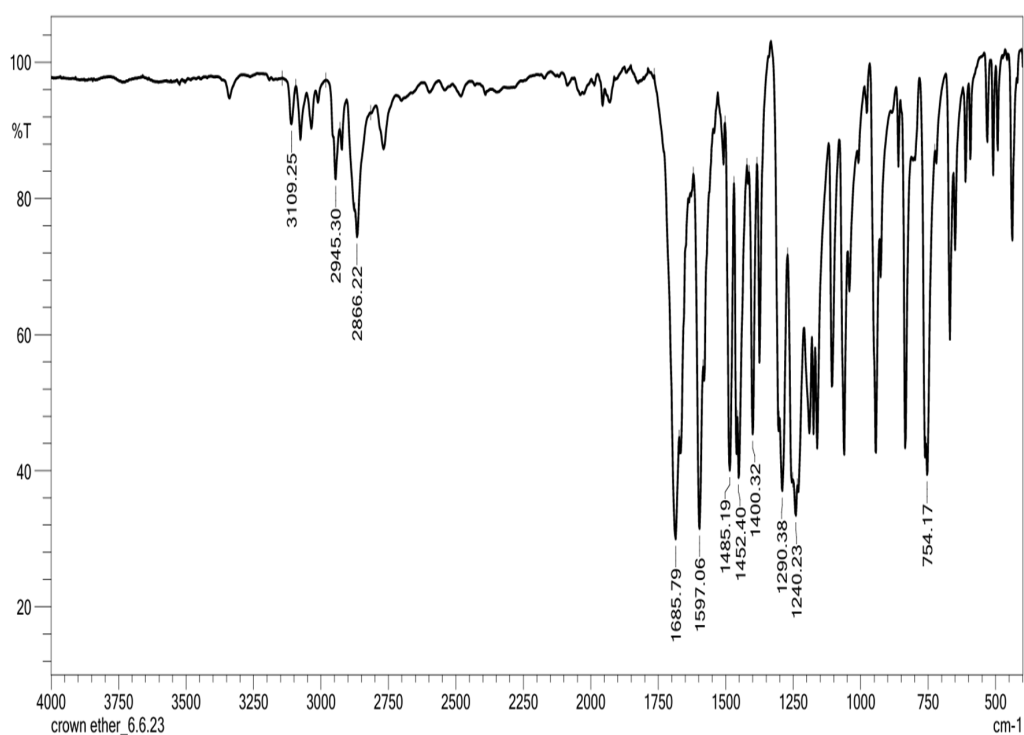


Figure S1. IR spectrum of Bis-aldehyde 3.

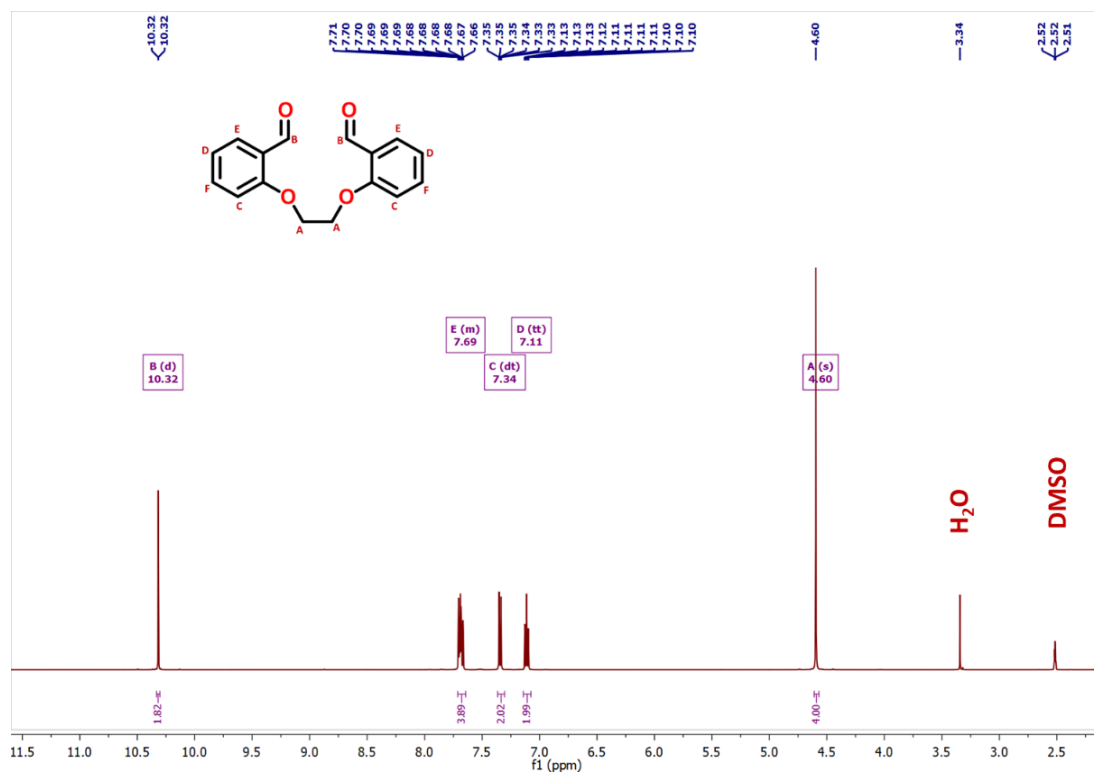


Figure S2. ¹H-NMR spectrum of Bis-aldehyde 3.

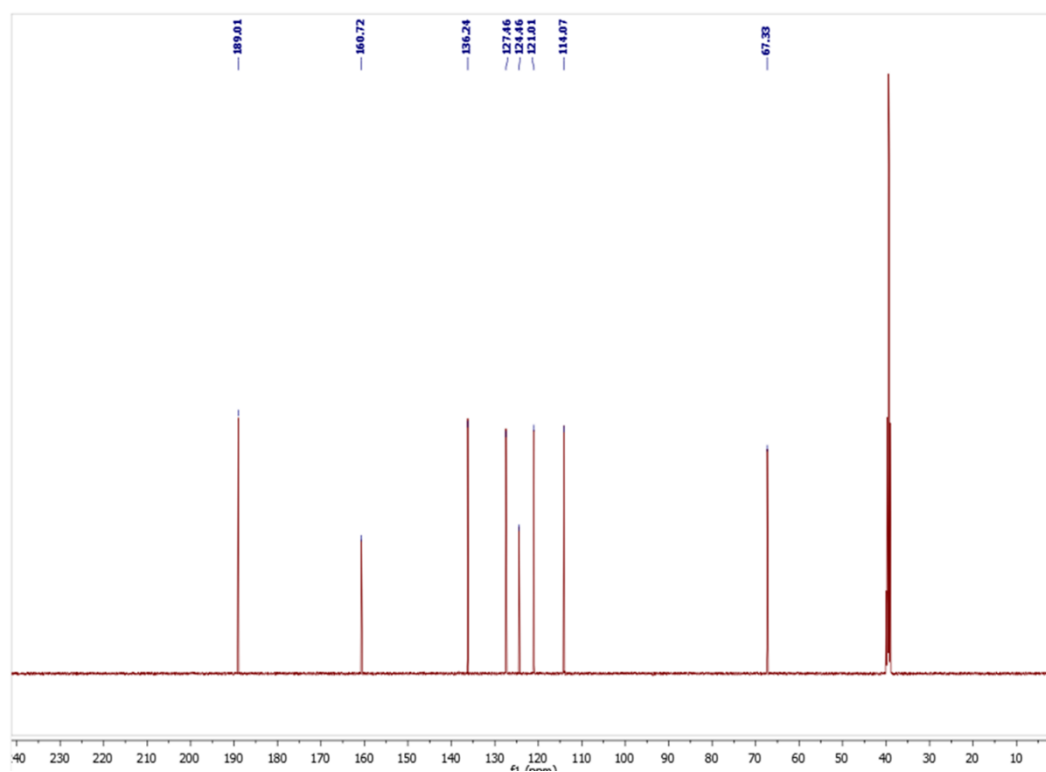


Figure S3. ¹³C-NMR spectrum of Bis-aldehyde 3.

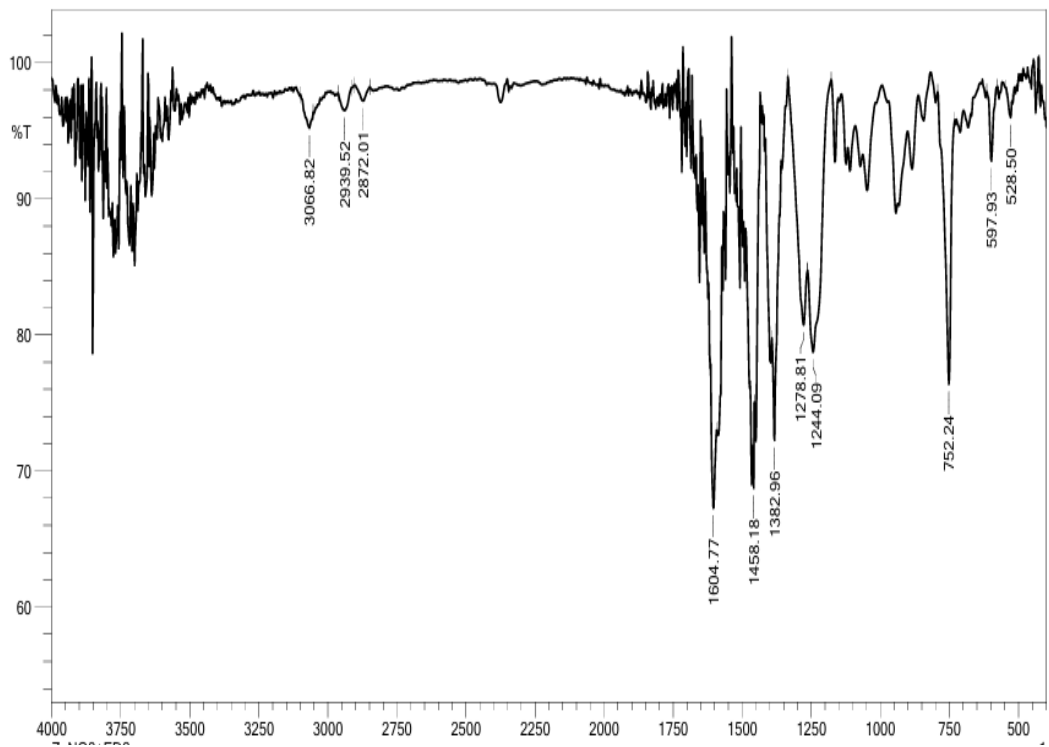


Figure S4. IR spectrum of complex 5a.

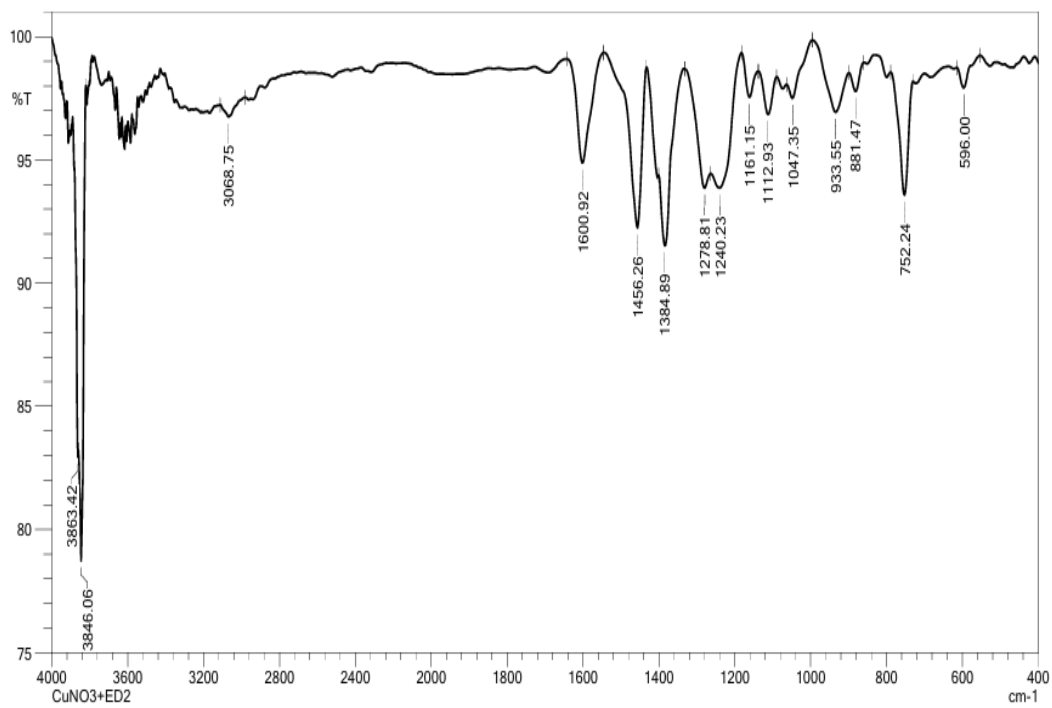


Figure S5. IR spectrum of complex 5b.

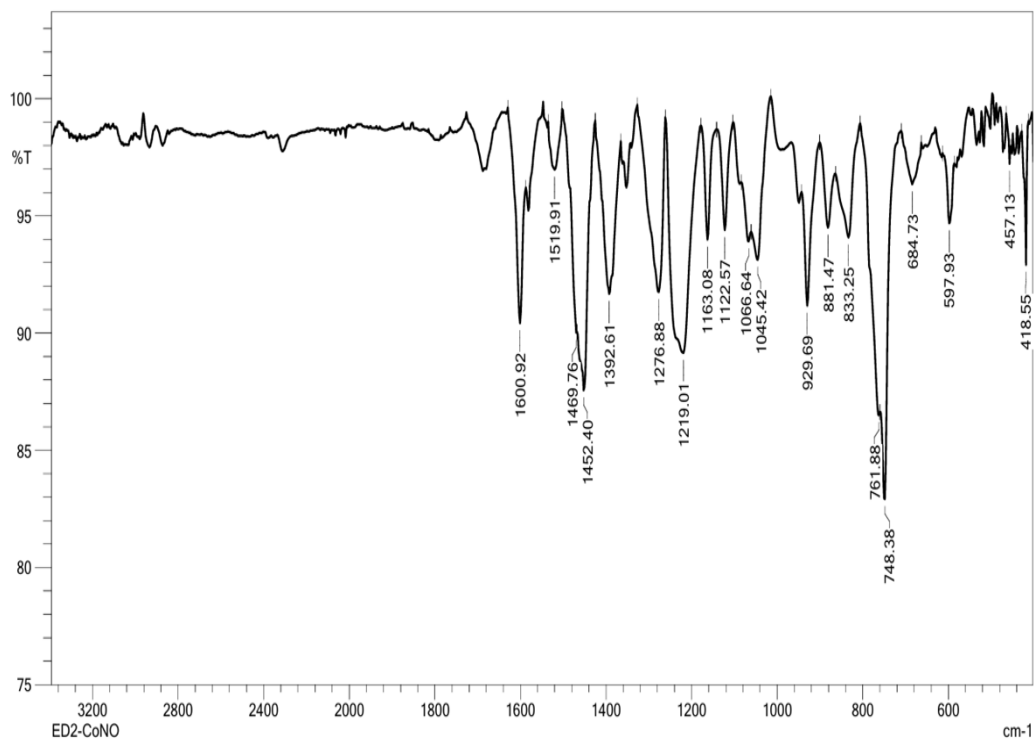


Figure S6. IR spectrum of complex 5c.

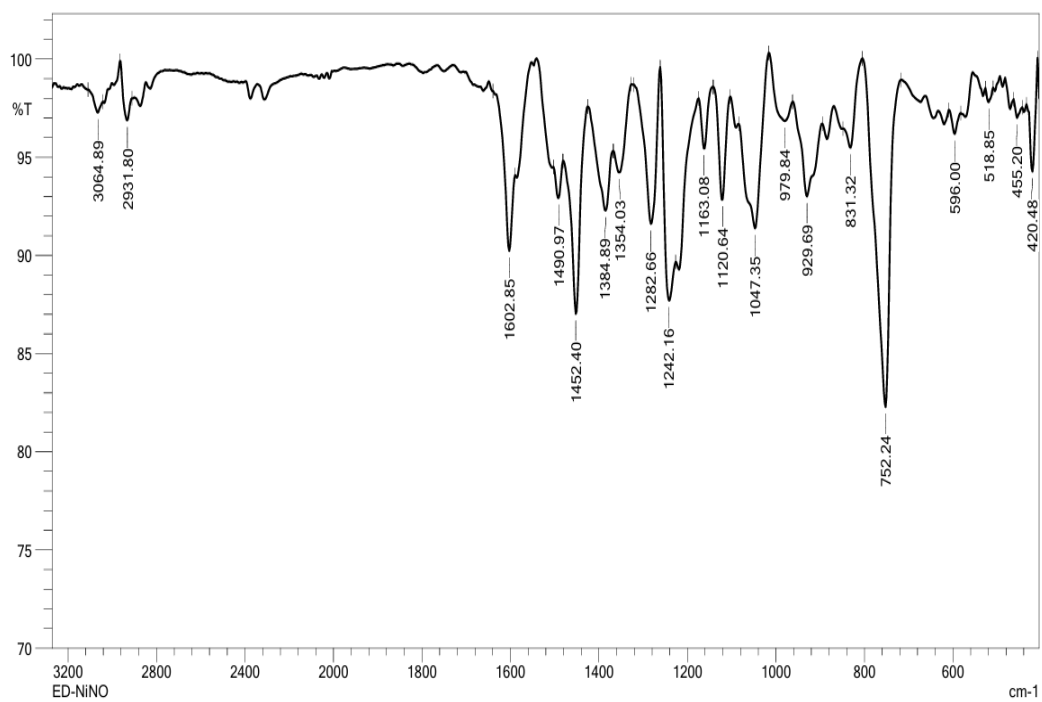


Figure S7. IR spectrum of complex 5d.

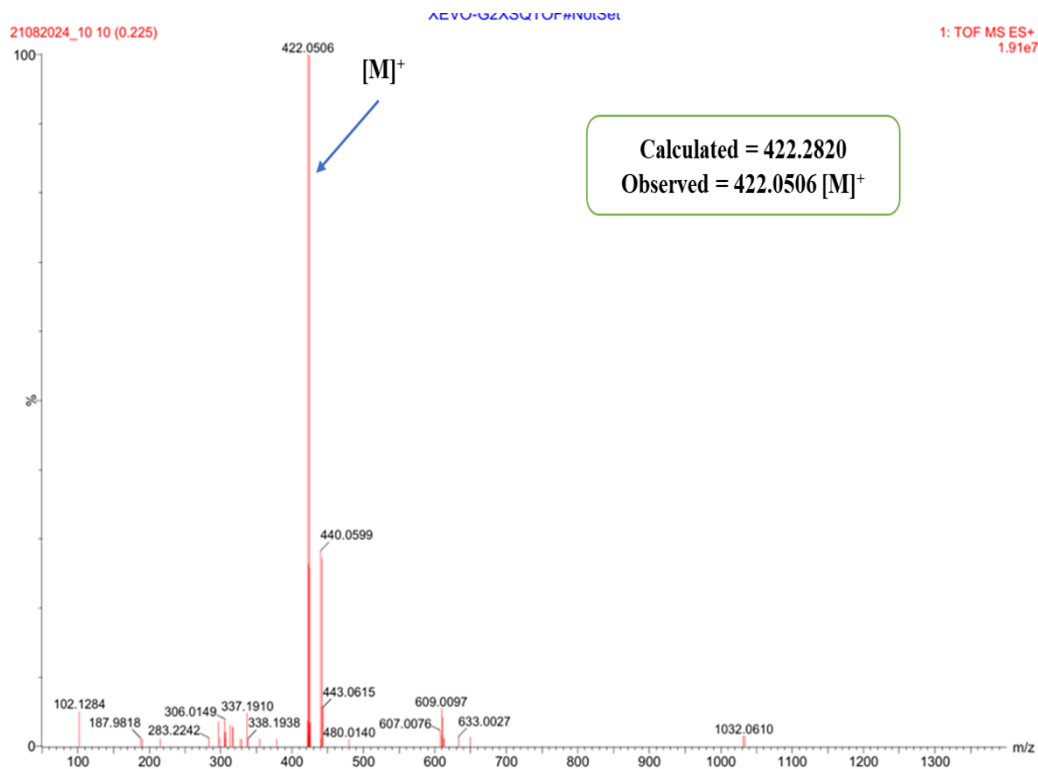


Figure S8. HRMS of ligand **4**.

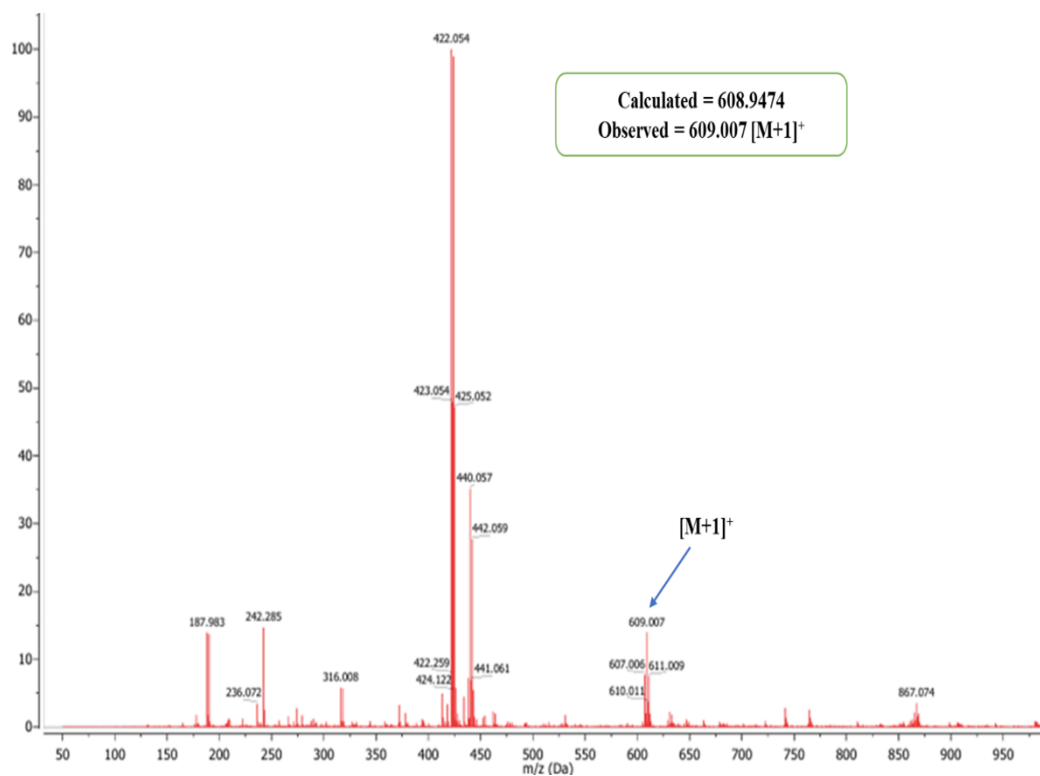


Figure S9. HRMS of complex **5a**.

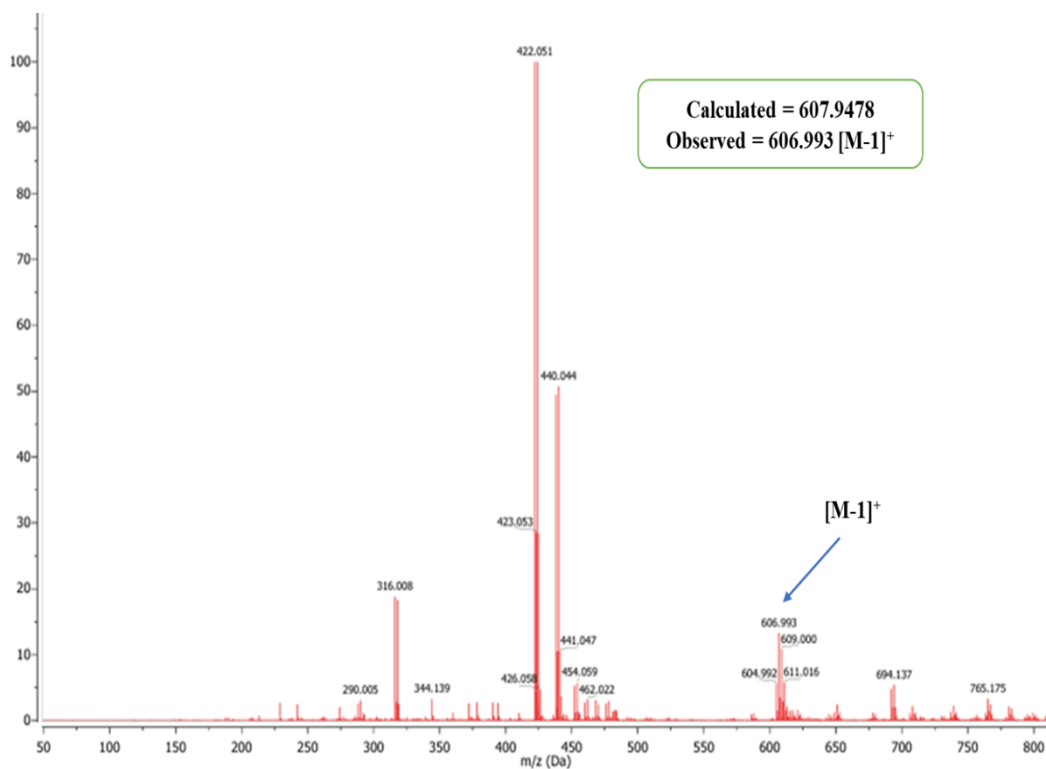


Figure S10. HRMS of complex 5b.

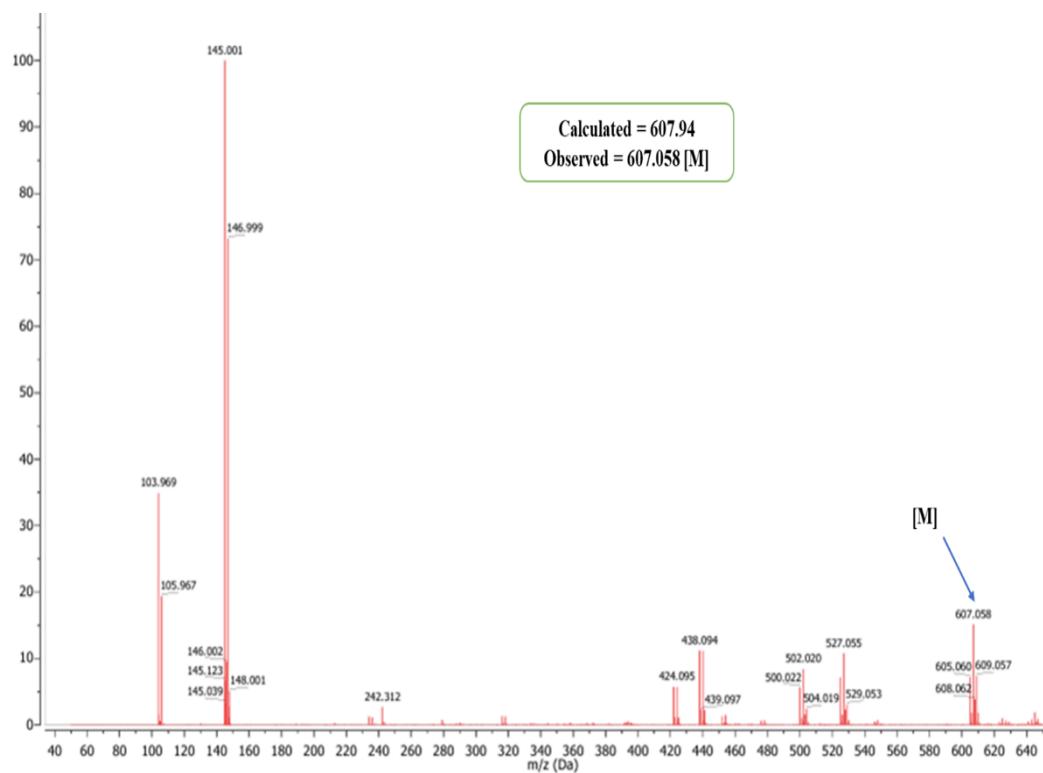


Figure S11. HRMS of complex 5c.

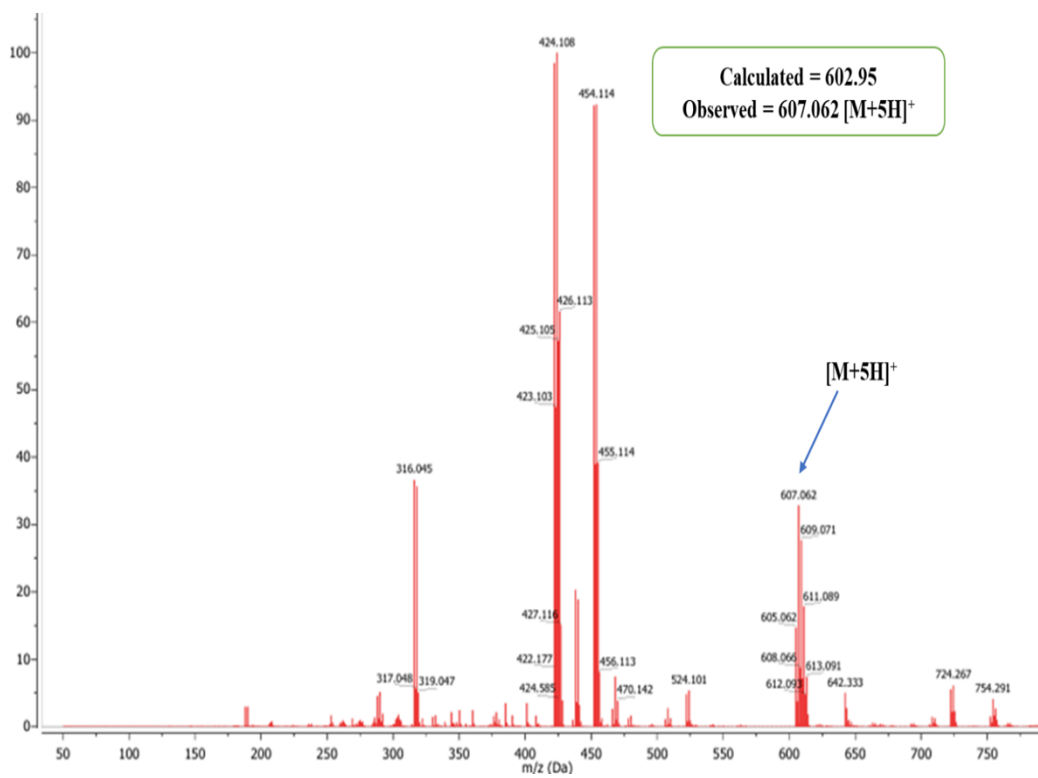


Figure S12. HRMS of complex **5d**.

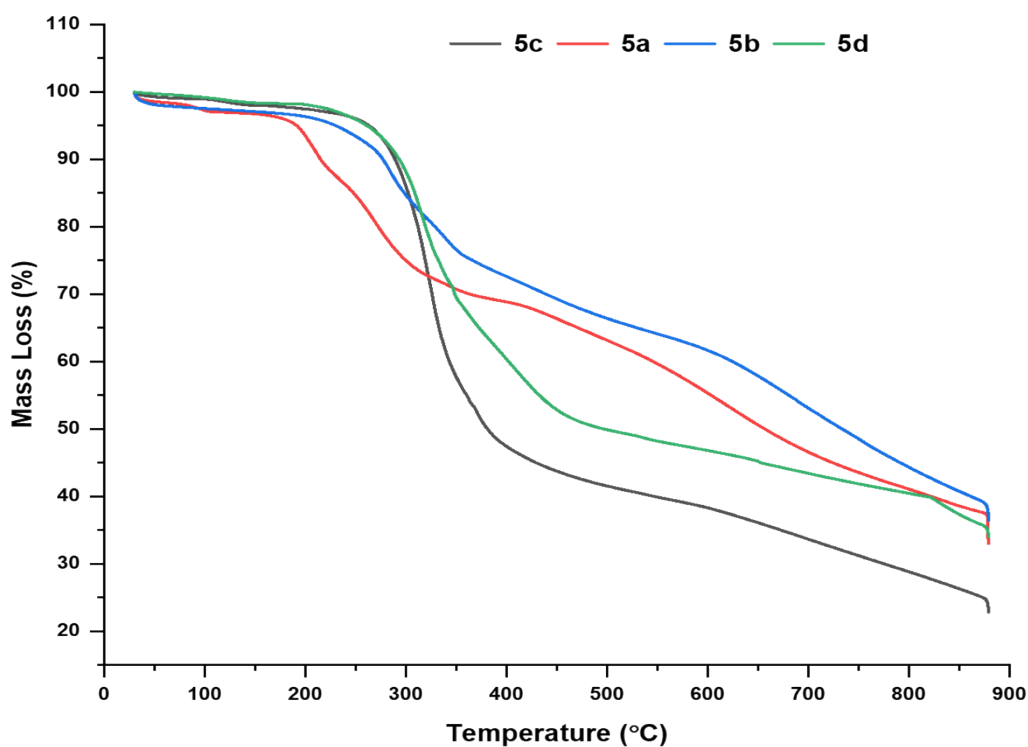


Figure S13. Thermograph of synthesized complexes (**5a-5d**).

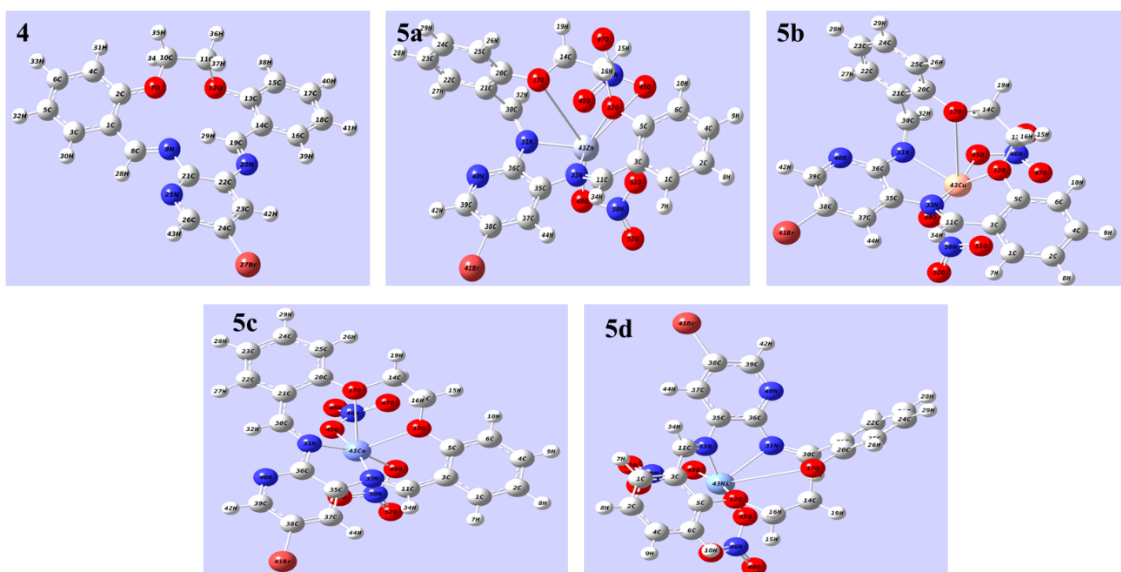


Figure S14. Optimized structures of synthesized compounds (4, 5a-5d).

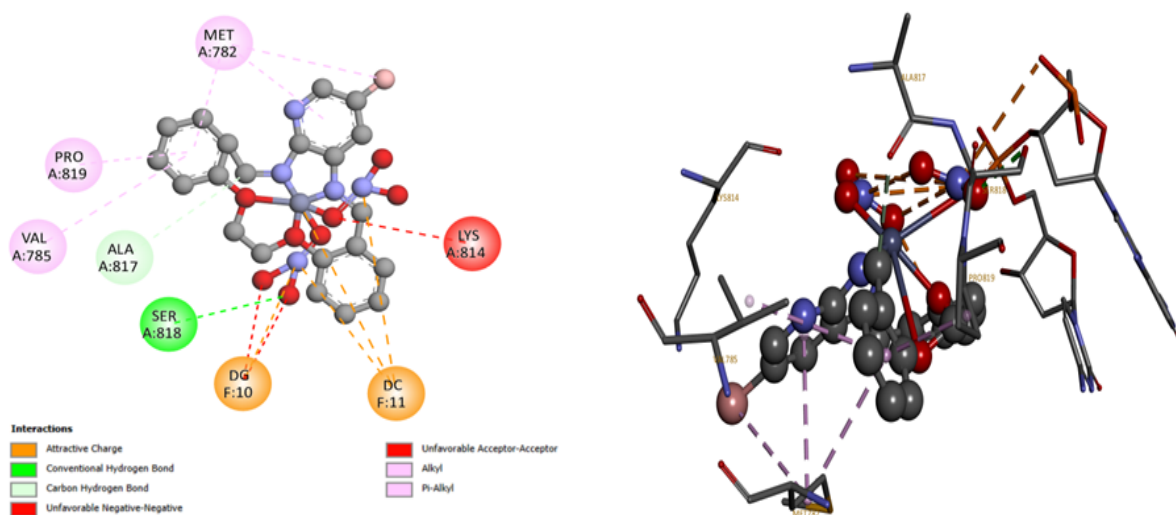


Figure S15. Interactions of complex 5a with active site of Topoisomerase II β protein docked by AutoDock Vina.

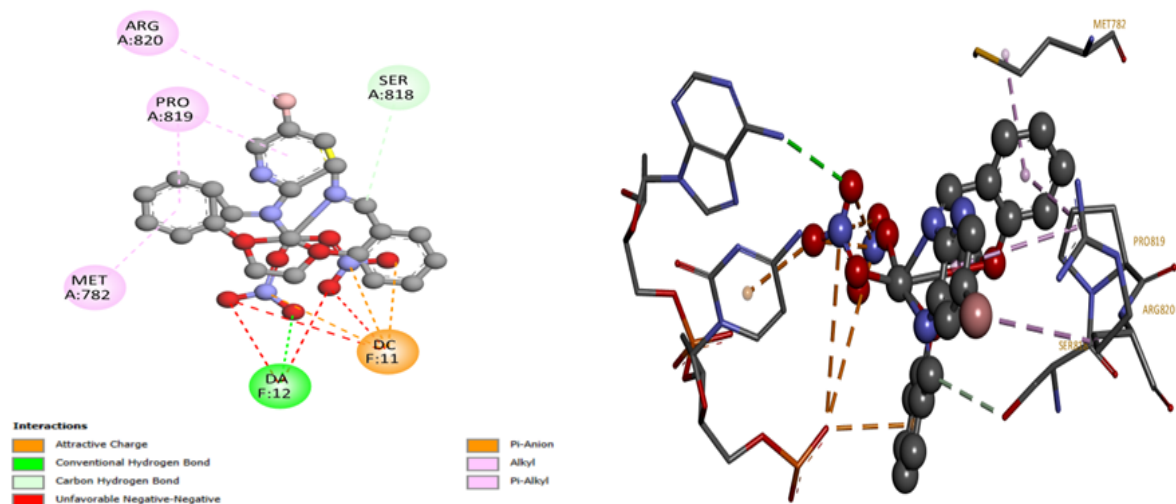


Figure S16. Interactions of complex **5b** with active site of Topoisomerase II β protein docked by AutoDock Vina.

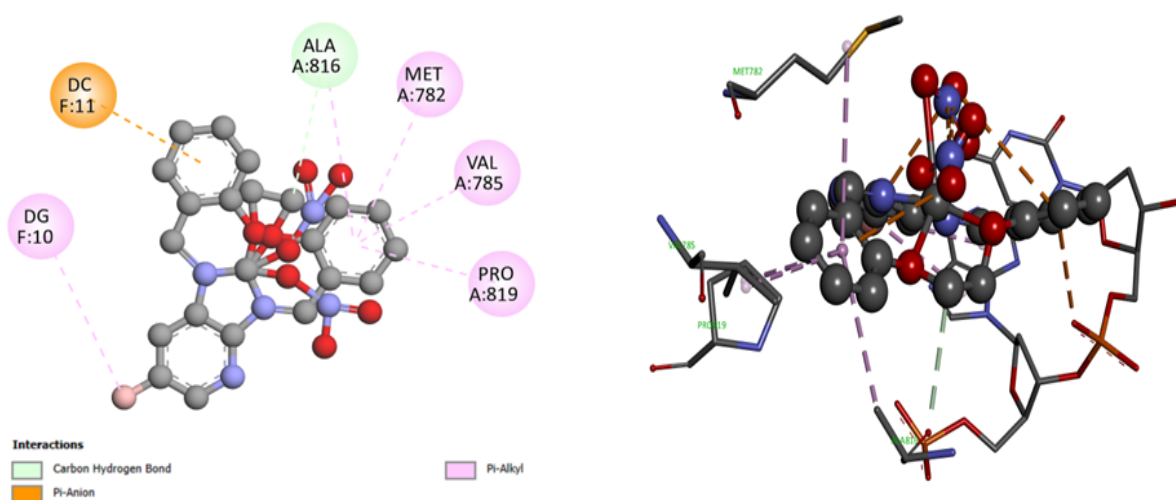


Figure S17. Interactions of complex **5c** with active site of Topoisomerase II β protein docked by AutoDock Vina.

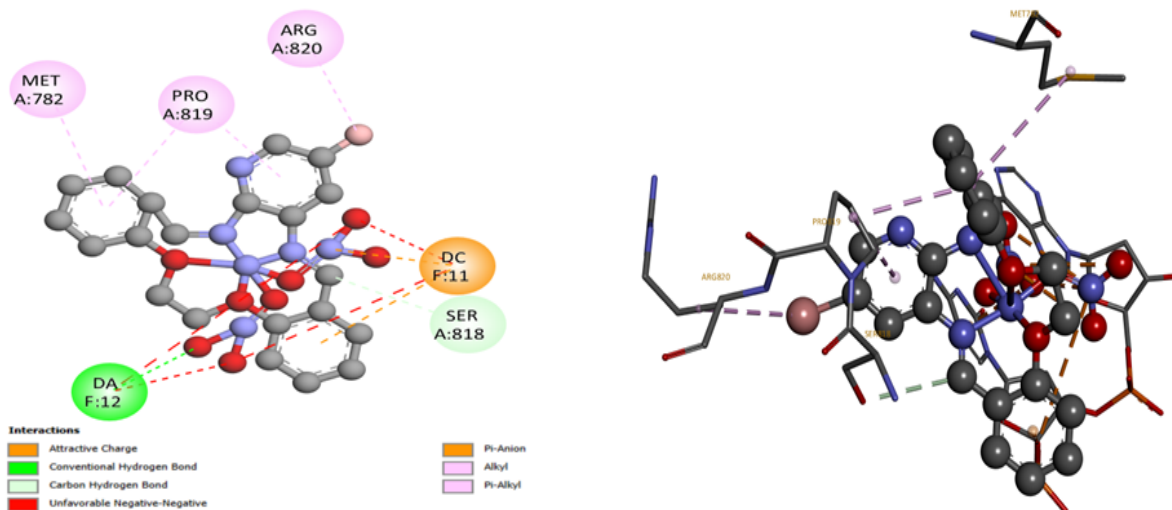


Figure S18. Interactions of complex **5d** with active site of Topoisomerase II β protein docked by AutoDock Vina.

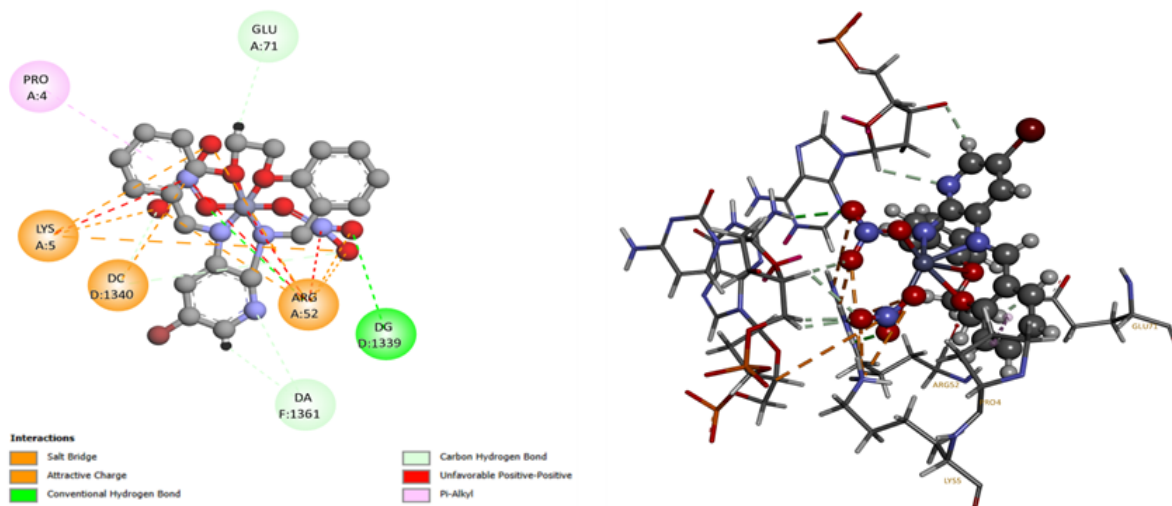


Figure S19. Interactions of complex **5a** with active site of Topoisomerase II β protein docked by GOLD.

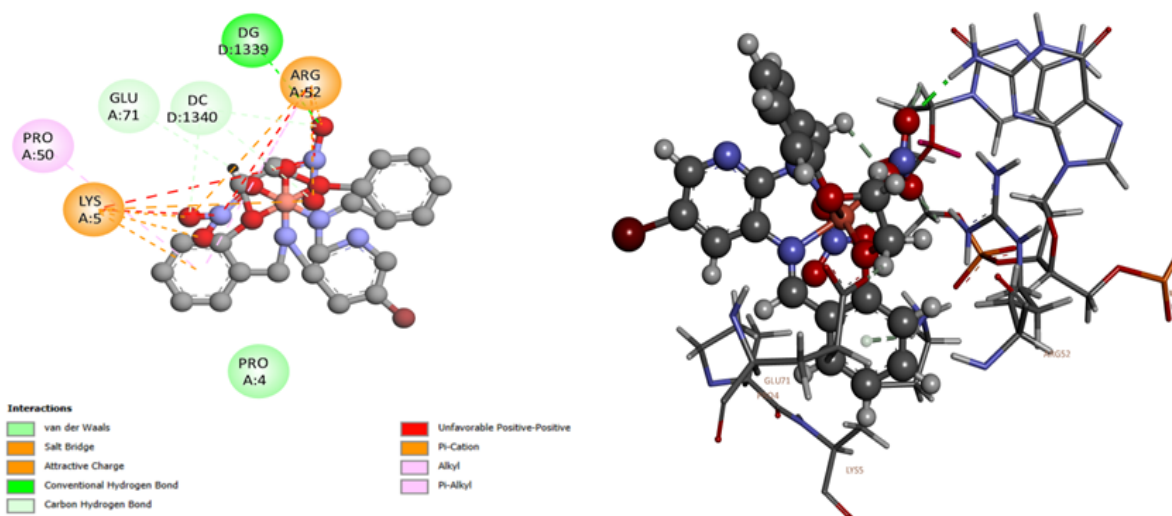


Figure S20. Interactions of complex **5b** with active site of Topoisomerase II β protein docked by GOLD.

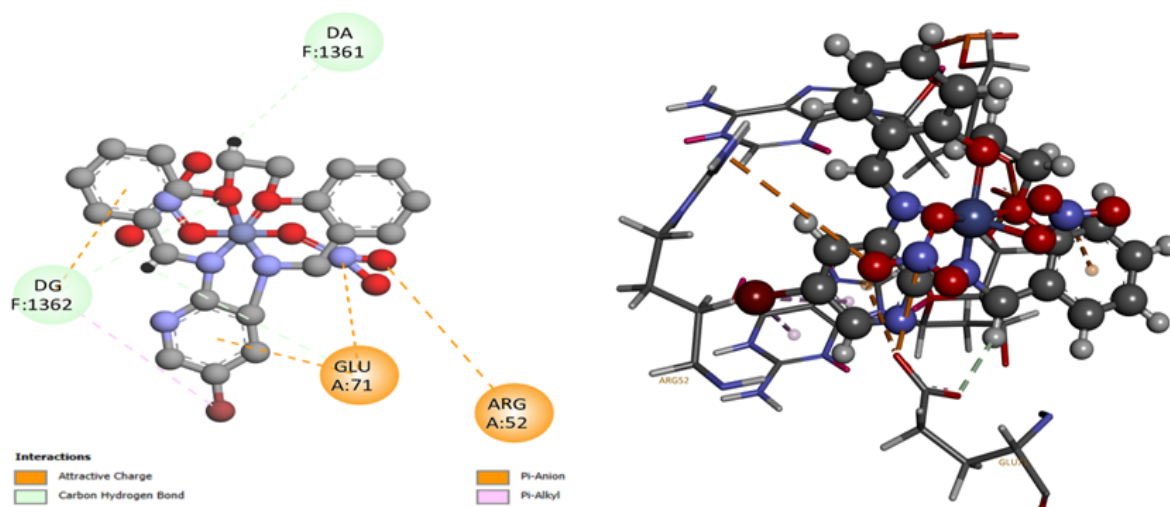


Figure S21. Interactions of complex **5c** with active site of Topoisomerase II β protein docked by GOLD.

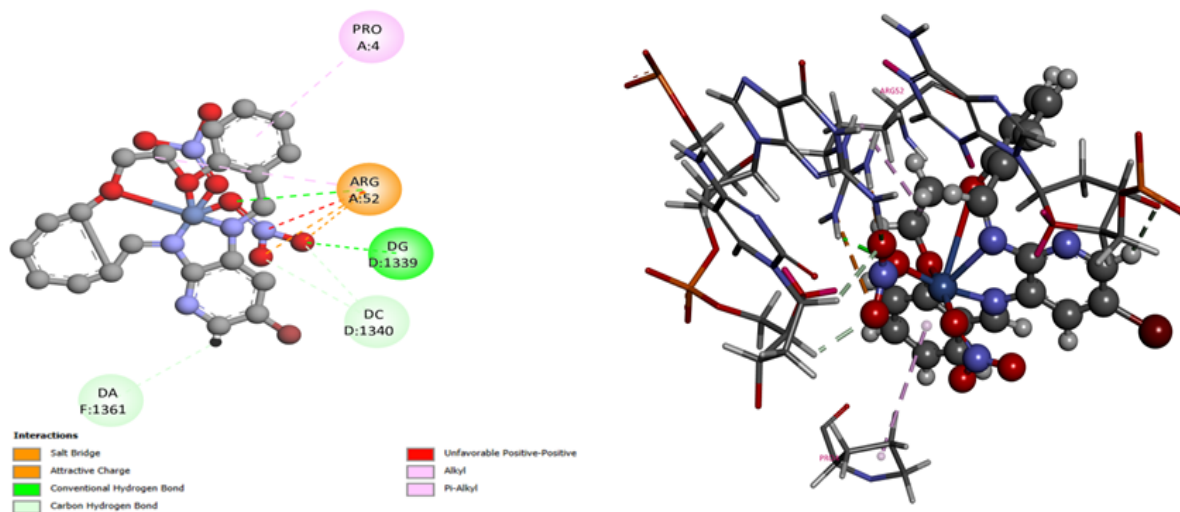


Figure S22. Interactions of complex **5d** with active site of Topoisomerase II β protein docked by GOLD.

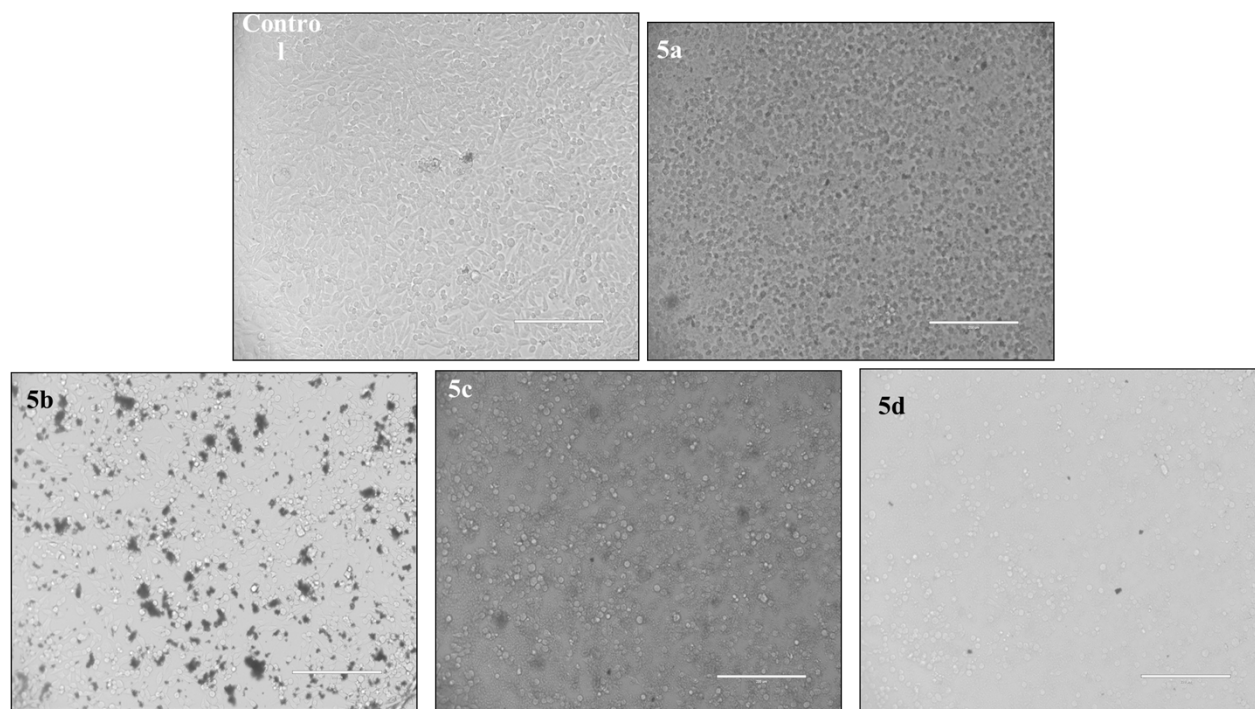


Figure S23. The morphological changes in cells after 24 hrs treatment with complexes **5a-5d**.

Table S1. Selected bond lengths of optimized structures of ligand **4** and its complexes **5a-5d**.

Bond Length (Å)	4	5a	5b	5c	5d
C (30) = N (31)	1.283	1.3	1.294	1.315	1.289
C (11) = N (33)	1.284	1.303	1.305	1.308	1.306
C (13) - O (12)	1.43	1.492	1.482	1.474	1.484
C (14) - O (17)	1.425	1.481	1.472	1.462	1.469
M (43) - N (31)	--	2.197	2.304	1.984	2.505
M (43) - N (33)	--	2.206	2.046	1.965	1.933
M (43) - NO₃⁻ (45)	--	3.316	1.953	1.923	1.888
M (43) - NO₃⁻ (49)	--	2.175	2.018	1.972	1.897
M (43) - O (12)	--	2.31	2.138	2.44	1.98
M (43) - O (17)	--	3.846	3.767	2.88	3.704

Table S2. Selective bond angles for optimized structures of complexes **5a-5d**.

Sr. No.	Bond Angle (°)	5a	5b	5c	5d
1.	A(O12, Zn43, O45)	66.67	94.96	114.53	94.75
2.	A(O12, Zn43, N31)	104.81	108.53	114.1	111.2
3.	A(O12, Zn43, N33)	74.34	80.07	78.32	85.44
4.	A(O12, Zn43, O49)	153.14	155.79	80.53	166.48
5.	A(O12, Zn43, O17)	52.06	50.40	61.30	50.36
6.	A(O17, Zn43, N31)	52.85	58.62	68.16	60.72
7.	A(O17, Zn43, O49)	146.158	150.26	128.47	140.95
8.	A(O17, Zn43, N33)	67.58	76.99	110.9	78.79
9.	A(O17, Zn43, O45)	99.25	88.15	76.83	92.99
10.	A(N31, Zn43, O49)	95.77	150.26	128.47	80.36
11.	A(N31, Zn43, N33)	75.54	77.46	83.27	77.49
12.	A(N31, Zn43, O45)	129.88	89.99	90.54	92.46
13.	A(O49, Zn43, N33)	94.79	92.63	91.92	90.53
14.	A(O49, Zn43, O45)	112.34	97.64	90.76	91.59
15.	A(Zn43, N33, C35)	111.6	114.64	107.44	117.23
16.	A(Zn43, N31, C36)	111.98	107.76	106.47	101.54
17.	A(Zn43, O12, C13)	135.07	129.81	127.17	129.68
18.	A(Zn43, O17, C14)	73.12	68.15	107.27	66.82

Table S3. Geometric parameters of H-bonds connecting the studied ligands to the receptor's active site obtained from AutoDock Vina and GOLD software.

AutoDock Vina				GOLD		
Ligand	Amino Acid	H-Bonds type	Bond Distance (Å)	Amino Acids	H-Bonds type	Bond Distance (Å)
4	GLN805	O---H-N	2.89	No H-Bond Interactions		
	ASP815	C-H---O	3.79			
	SER480	C-H---O	3.42			
	SER483	C---H-O	4.01			
	DG10	C-H---O	3.45			
5a	SER818	O-H---O	2.83	DG1339	O---H-N	2.68
	ALA817	O---H-C	3.79	GLU71	C-H---O	4.28
5b	DA12	O---H-N	3.13	ARG52	O---H-C	2.01
	SER818	C-H---O	3.59	DC1340	O---H-C	2.63
				DA1361	N---H-C	2.83
5c				GLU71	C-H---O	2.26
				DC1340	O---H-C	2.30
				DG1339	O---H-N	2.11
5d	ALA816	C-H---O	3.79	GLU71	C-H---O	2.70
				DG1362	O---H-C	2.24
				DA1361	C-H---O	3.00
5d	DA12	O---H-N	3.08	DA1361	C-H---O	2.91
	SER818	C-H---O	3.80	ARG52	O---H-N	2.07
				DG1339	O---H-N	1.69
				DC1340	O---H-C	2.26

Table S4. Toxicity of synthesized compounds.

Sr. No.	Compound	IC ₅₀ (µM)
1.	4	0.09
2.	5a	0.12
3.	5b	0.1
4.	5c	0.1
5.	5d	0.13
6.	DOX	0.02